modelling

MDPI

Article

Modeling of a Fluid with Pressure-Dependent Viscosity in Hele-Shaw Flow

Benedetta Calusi [1,*] and Liviu Iulian Palade [2]

[1] Dipartimento di Matematica e Informatica "Ulisse Dini", Università degli Studi di Firenze, Viale Morgagni 67/a, 50134 Firenze, Italy
[2] Institut Camille Jordan CNRS UMR 5208, INSA-Lyon & Pôle de Mathématiques, Université de Lyon, 21 Avenue Jean Capelle, 69621 Villeurbanne Cedex, France; liviu-iulian.palade@insa-lyon.fr
* Correspondence: benedetta.calusi@unifi.it

Abstract: We investigate the Hele-Shaw flow of fluids whose viscosity depends on pressure, i.e., piezo-viscous fluids, near the tip of a sharp edge. In particular, we consider both cases of two-dimensional symmetric and antisymmetric flows. To obtain the pressure field, we provide a procedure that is based on the method of separation of variables and does not depend on a specific choice of the expression for the pressure-dependent viscosity. Therefore, we show the existence of a general procedure to investigate the behavior of piezo-viscous fluids in Hele-Shaw flow and its solution near a sharp corner. The results are applied to the case of an exponential dependence of viscosity on pressure as an example of exact solutions for the pressure field.

Keywords: Hele-Shaw flow; symmetrical and antisymmetrical flows; lubrication approximation; pressure-dependent viscosity; piezo-viscous fluids

check for updates

Citation: Calusi, B.; Palade, L.I. Modeling of a Fluid with Pressure-Dependent Viscosity in Hele-Shaw Flow. *Modelling* **2024**, *5*, 1490–1504. https://doi.org/10.3390/modelling5040077

Academic Editor: Sergey Utyuzhnikov

Received: 31 July 2024
Revised: 25 September 2024
Accepted: 30 September 2024
Published: 9 October 2024

1. Introduction

Hele-Shaw flow refers to the flow in a narrow gap between two parallel plates. The space between the plates can be occupied partly by the fluid and partly by internal obstacles placed perpendicular to the flow direction. Such obstacles can have different geometry such as cylinders with generators perpendicular to the plates [1] or sharp edges [2]. The study on the flow between two parallel plates close together is a relevant problem, e.g., for micro-flow and industrial applications such as injection molding of thin films [2]. In fact, several applications in geophysical, biological, and industrial fields involves complex fluids flowing in domains that can be approximated as an incline or two parallel plates; thus, the modeling of such fluids is of great interest, and various works have been developed on this topic [3–22]. In the early studies, Hele-Shaw flow was applied to Newtonian fluids, and it is named after Henry Selby Hele-Shaw, who studied the problem in 1898 [23]. Later, extensions of Hele-Shaw flow for non–Newtonian fluids were analyzed (see, e.g., [1,2,24–27] and the references therein). The Hele-Shaw flows of a power law fluid around sharp corners were analyzed, e.g., in [1,24]. Recently, more complex viscosity laws have been considered. In ref. [26], the Hele-Shaw flow equations for both viscous and viscoplastic fluids have been investigated through a viscometric fluidity function. The authors of [2] have extended the analysis of Hele-Shaw flow around a sharp edge whose tip is assumed a geometric singularity for generalized Newtonian fluids and yield stress fluids.

The purpose of this work is to present the two-dimensional Hele-Shaw flow applied to a piezo-viscous fluid, i.e., a fluid whose viscosity depends on the pressure, in the case of both antisymmetric (perpendicular to the edge axis of symmetry) and symmetric (directed towards the edge and parallel to the axis of symmetry) flows.

In particular, we extend the procedure presented in [2] to the case of piezo-viscous fluids by looking for a solution of the pressure field in an area of a sharp edge, as depicted in Figure 1. Several studies have been developed to investigate the flow of fluids with viscosity,

which depends on pressure, e.g., see [28–37]. The authors of [30] have studied the Falkner–Skan boundary layer flow of a non–Newtonian fluid whose viscosity follows the Barus' law [28], i.e., the fluid is characterized by an exponential relationship between viscosity and pressure. To the best of the authors' knowledge, Hele-Shaw flow has never been extended before to piezo-viscous fluids in the case of both antisymmetric and symmetric flows without a specific reference to the explicit dependence of viscosity on pressure. This paper is organized as follows. In Section 2, we provide the governing equations for piezo-viscous fluids in a narrow gap between two parallel plates and, then, the differential equations for the pressure field through the method of separation of variables. In Section 3, we investigate the pressure behavior in an area of a sharp edge, in a system of polar coordinates centered at the edge tip, for both symmetric and antisymmetric flows by considering generic pressure-dependent viscosity. Then, we provide the exact solutions for the pressure field in the case of an exponential dependence of viscosity on pressure. Section 4 is devoted to final remarks and future developments.

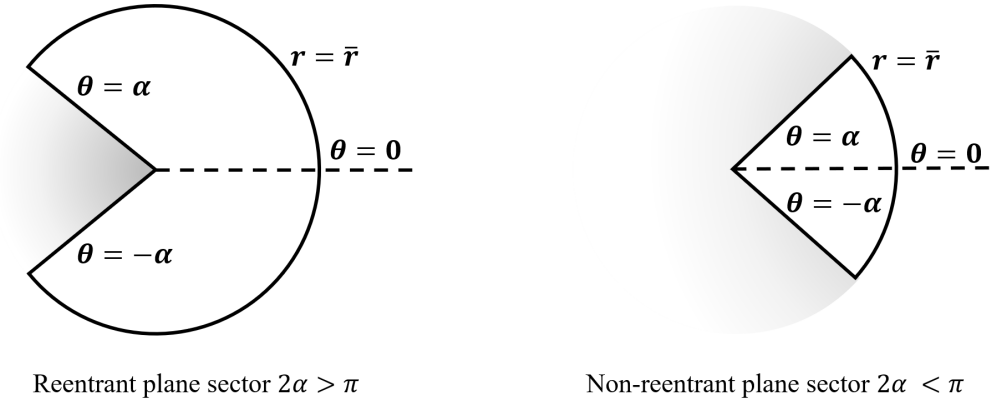

Reentrant plane sector $2\alpha > \pi$ Non-reentrant plane sector $2\alpha < \pi$

Figure 1. Sketches of the problem geometry when the edge angle is such that the region close to the tip is a sharp edge (re-entrant plane sector) or a hollow-shaped cavity (non re-entrant plane sector).

2. Mathematical Background

We consider a fluid with pressure-dependent viscosity, $f^*(p^*)$, characterized by the following constitutive relation:

$$\mathbb{S}^* = 2f^*(p^*)\boldsymbol{A}_1^*, \tag{1}$$

where $\mathbb{S}^*$ is the Cauchy extra-stress tensor and $\boldsymbol{A}_1^*$ is the (traceless) first Rivlin–Eriksen tensor, as follows:

$$\boldsymbol{A}_1^* = \frac{1}{2}\left[\nabla \boldsymbol{u}^* + (\nabla \boldsymbol{u}^*)^T\right], \tag{2}$$

with $\boldsymbol{u}^*$ being the velocity field. The general forms of governing equations are

$$\begin{cases} \rho^*\left(\dfrac{\partial \boldsymbol{u}^*}{\partial t^*} + \boldsymbol{u}^* \cdot \nabla \boldsymbol{u}^*\right) = -\nabla p^* + \mathrm{div}\mathbb{S}^*, \\ \\ \mathrm{div}\boldsymbol{u}^* = 0, \end{cases} \tag{3}$$

where ρ^* is the constant fluid density. We consider the velocity field of the form

$$\boldsymbol{u}^*(x^*, y^*, z^*) = u^*(x^*, y^*, z^*)\boldsymbol{e}_x^* + v^*(x^*, y^*, z^*)\boldsymbol{e}_y^* + w^*(x^*, y^*, z^*)\boldsymbol{e}_z^*, \tag{4}$$

and the gap between the horizontal x^*Oy^* plane and any of the two boundary planes to be denoted as $|z^*| = H^*/2$. The schematic diagram is displayed in Figure 2.

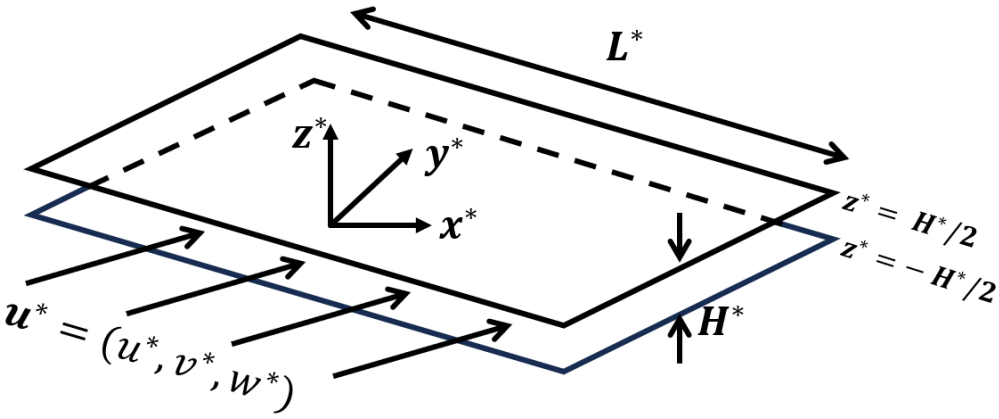

Figure 2. Schematic diagram of the three-dimensional flow domain geometry.

We consider the following boundary conditions:

$$\boldsymbol{u}^* = 0, \qquad \text{for } z^* = \pm\frac{H^*}{2}, \tag{5}$$

i.e., the no wall slip condition, and, due to the flow domain symmetry,

$$\frac{\partial u^*}{\partial z^*} = \frac{\partial v^*}{\partial z^*} = 0, \qquad \text{for } z^* = 0, \tag{6}$$

i.e., we focus only on the upper half subdomain $z^* \in [0, H^*/2]$. For Hele-Shaw flows, the fluid film thickness is negligible compared to the domain $x^* - y^*$ of other dimensions. Since the flow is chiefly confined to the x^* and y^* directions, it is usually assumed that w^* is negligible compared to u^* and v^*.

We introduce the following dimensionless quantities:

$$\begin{gathered} x = \frac{x^*}{L^*}, \quad y = \frac{y^*}{L^*}, \quad z = \frac{z^*}{H^*}, \quad u = \frac{u^*}{U^*_{ref}}, \quad v = \frac{v^*}{U^*_{ref}}, \quad w = \frac{w^*}{\epsilon U^*_{ref}}, \\ t = \frac{U^*_{ref}}{L^*}t^*, \quad p = \frac{p^* - p^*_0}{p^*_c}, \quad \mathbb{S} = \frac{\mathbb{S}^*}{S^*_c}, \quad f(p) = \frac{f^*(p^*)}{\mu^*_0}, \end{gathered} \tag{7}$$

with

$$\epsilon = \frac{H^*}{L^*} \ll 1, \tag{8}$$

$$p^*_c = \frac{\mu^*_0 U^*_{ref} L^*}{H^{*2}}, \qquad S^*_c = \frac{\mu^*_0 U^*_{ref}}{H^*}, \tag{9}$$

where U^*_{ref} is the reference velocity, p^*_c is the characteristic pressure, μ^*_0 is the fluid viscosity evaluated at the reference pressure p^*_0, and L^* is the domain length in the x^* and y^* directions. Introducing the Reynolds number as

$$\mathrm{Re} = \frac{\rho^* U^*_{ref} H^*}{\mu^*_0}, \tag{10}$$

as well as using (4) and adimensionalization (7), system (3) rewrites the equation as follows:

$$\begin{cases} \epsilon \mathsf{Re}\left(u\dfrac{\partial u}{\partial x}+v\dfrac{\partial u}{\partial y}+w\dfrac{\partial u}{\partial z}\right)=-\dfrac{\partial p}{\partial x}+\left\{2\epsilon^2\dfrac{\partial}{\partial x}\left(f(p)\dfrac{\partial u}{\partial x}\right)+\epsilon^2\dfrac{\partial}{\partial y}\left[f(p)\left(\dfrac{\partial v}{\partial x}\right.\right.\right. \\ \qquad\qquad \left.\left.\left.+\dfrac{\partial u}{\partial y}\right)\right]+\dfrac{\partial}{\partial z}\left[f(p)\left(\epsilon^2\dfrac{\partial w}{\partial x}+\dfrac{\partial u}{\partial z}\right)\right]\right\}, \\ \epsilon \mathsf{Re}\left(u\dfrac{\partial v}{\partial x}+v\dfrac{\partial v}{\partial y}+w\dfrac{\partial v}{\partial z}\right)=-\dfrac{\partial p}{\partial y}+\epsilon^2\dfrac{\partial}{\partial x}\left[f(p)\left(\dfrac{\partial v}{\partial x}+\dfrac{\partial u}{\partial y}\right)\right] \\ \qquad\qquad +2\epsilon^2\dfrac{\partial}{\partial y}\left(f(p)\dfrac{\partial v}{\partial y}\right)+\dfrac{\partial}{\partial z}\left[f(p)\left(\dfrac{\partial v}{\partial z}+\epsilon^2\dfrac{\partial w}{\partial x}\right)\right], \\ \epsilon^2 \mathsf{Re}\left(u\dfrac{\partial w}{\partial x}+v\dfrac{\partial w}{\partial y}+w\dfrac{\partial w}{\partial z}\right)=-\dfrac{\partial p}{\partial z}+\dfrac{\partial}{\partial x}\left[f(p)\left(\epsilon\dfrac{\partial u}{\partial z}+\epsilon^3\dfrac{\partial w}{\partial x}\right)\right] \\ \qquad\qquad +\dfrac{\partial}{\partial y}\left[f(p)\left(\epsilon\dfrac{\partial v}{\partial z}+\epsilon^3\dfrac{\partial w}{\partial y}\right)\right]+2\epsilon\dfrac{\partial}{\partial z}\left(f(p)\dfrac{\partial w}{\partial z}\right). \end{cases} \tag{11}$$

By assuming that $\mathsf{Re}=\mathcal{O}(1)$ and neglecting a higher order than ϵ, system (11) reduces to

$$\begin{cases} \dfrac{\partial p}{\partial x}=\dfrac{\partial}{\partial z}\left(f(p)\dfrac{\partial u}{\partial z}\right), \\ \dfrac{\partial p}{\partial y}=\dfrac{\partial}{\partial z}\left(f(p)\dfrac{\partial v}{\partial z}\right), \\ \dfrac{\partial p}{\partial z}=0, \\ \dfrac{\partial u}{\partial x}+\dfrac{\partial v}{\partial y}+\dfrac{\partial w}{\partial z}=0. \end{cases} \tag{12}$$

Remark 1. *We consider the following explicit form for the dimensional viscosity $f^*(p^*)$ as proposed by Barus in* [28]*, namely*

$$f^*(p^*)=\mu_0^* e^{\delta^*(p^*-p_0^*)}, \qquad p^*=p^*(x^*,y^*,z^*), \tag{13}$$

where μ_0^* is the viscosity at the reference pressure p_0^* and δ^* is the pressure coefficient. Then, by considering adimensionalization (7)*, we have*

$$f(p)=e^{\delta p}, \qquad \text{where} \quad \delta=\delta^* p_c^*=\frac{\delta^*\mu_0^* U_{ref}^* L^*}{H^{*2}}, \tag{14}$$

which is a positive and increasing function of pressure [38,39]*, and δ is a "material" and a geometrical parameter proportional to the pressure coefficient δ^*. The classical Newtonian case is recovered for $\delta^*\to 0$. Figure 3 shows the schematic representation of $f(p)$ for classical Newtonian fluid and piezo-viscous fluids with viscosity given by* (14)*.*

System (12) is to be coupled with boundary conditions (6), which take the following forms in a dimensionless formulation:

$$\boldsymbol{u}=0, \qquad \text{for } z=\pm\frac{1}{2}, \tag{15}$$

and

$$\frac{\partial u}{\partial z}=\frac{\partial v}{\partial z}=0, \qquad \text{for } z=0. \tag{16}$$

System (12) entails

$$p=p(x,y), \tag{17}$$

and, thus, Equation $(12)_{1,2}$ become

$$\begin{cases} \dfrac{\partial p}{\partial x} = f(p)\dfrac{\partial^2 u}{\partial z^2}, \\ \\ \dfrac{\partial p}{\partial y} = f(p)\dfrac{\partial^2 v}{\partial z^2}, \end{cases} \tag{18}$$

which, recalling conditions (15) and (16), lead to

$$\begin{cases} u(x,y,z) = \dfrac{1}{f(p(x,y))}\dfrac{\partial p(x,y)}{\partial x}\left(\dfrac{z^2}{2} - \dfrac{1}{8}\right), \\ \\ v(x,y,z) = \dfrac{1}{f(p(x,y))}\dfrac{\partial p(x,y)}{\partial y}\left(\dfrac{z^2}{2} - \dfrac{1}{8}\right), \end{cases} \tag{19}$$

i.e., the velocity field is symmetric about $z = 0$ and has a parabolic profile with respect to z. Moreover, following [2], we can write the flow fluxes q_u and q_v as

$$q_u(x,y) = 2\int_0^{1/2} u(x,y,z)dz = -\frac{1}{12f(p)}\frac{\partial p}{\partial x}, \tag{20}$$

$$q_v(x,y) = 2\int_0^{1/2} v(x,y,z)dz = -\frac{1}{12f(p)}\frac{\partial p}{\partial y}. \tag{21}$$

The flow fluxes in Equations (20) and (21) must satisfy

$$\frac{\partial q_u}{\partial x} + \frac{\partial q_v}{\partial y} = 0, \tag{22}$$

leading to a close equation for pressure, namely

$$\frac{\partial}{\partial x}\left[g(f(p))\frac{\partial p}{\partial x}\right] + \frac{\partial}{\partial y}\left[g(f(p))\frac{\partial p}{\partial y}\right] = \mathrm{div}[g(f(p))\nabla p] = 0, \tag{23}$$

where

$$g(f(p)) = \frac{1}{12f(p)}. \tag{24}$$

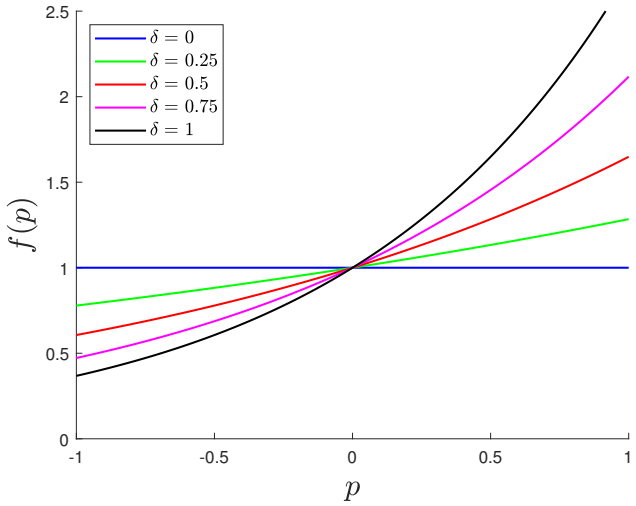

Figure 3. Plot of $f(p)$ as a function of p for classical Newtonian fluid (blue line) and piezo−viscous fluids given by (14) for different values of δ.

Remark 2. *The classical Newtonian case is retrieved when* $f^*(p^*) = \mu_0^* =$ *constant in a dimensional formulation, as follows:*

$$g^*(f^*(p^*)) = \frac{{H^*}^3}{12\mu_0^*}, \tag{25}$$

and, thus, Equation (23) *reduces to the well-known Reynolds equation, i.e.,*

$$\operatorname{div}\left[\frac{{H^*}^3}{12\mu_0^*}\nabla p^*\right] = 0, \tag{26}$$

which is essentially Equation (23) *with* $f(p) = 1$.

We rewrite (23) as

$$\operatorname{div}\left[\nabla\int_0^{p(x,y)} g(f(s))ds\right] = \operatorname{div}\left[\nabla\int_0^{p(x,y)}\frac{ds}{f(s)}\right] = \Delta\left[\int_0^{p(x,y)}\frac{ds}{f(s)}\right] = \Delta F(x,y) = 0, \tag{27}$$

which can be solved using the method of separation of variables.

3. Solution near the Corner Edge: General Case

In the region neighboring the edge (singularity) peak with a tip angle (constant in time) equal to 2α, looking for a solution via the separation of variables, i.e.,

$$F(r,\theta) = \int_0^{p(r,\theta)}\frac{ds}{f(s)} = R(r)\Theta(\theta), \tag{28}$$

we express Equation (23) in polar coordinates (r,θ), with their axis centered at the edge peak, namely

$$\frac{\partial}{\partial r}\left[r\frac{\partial}{\partial r}(R(r)\Theta(\theta))\right] + \frac{1}{r}\frac{\partial^2}{\partial\theta^2}(R(r)\Theta(\theta)) = 0, \quad (r,\theta)\in\mathbb{R}_+\times[-\alpha,\alpha]. \tag{29}$$

Therefore, by denoting the "separation constant" by m^2, Equation (29) entails

$$\begin{cases} \dfrac{r}{R}\dfrac{d}{dr}\left(r\dfrac{dR(r)}{dr}\right) = m^2, \\[2ex] \dfrac{d^2\Theta(\theta)}{d\theta^2}\dfrac{1}{\Theta(\theta)} = -m^2. \end{cases} \tag{30}$$

Following [24], since the dependence of viscosity on the shear rate $\dot{\gamma}$ is linear (i.e., the power law index, n, is equal to 1 in [24]), the problem is to find the smallest eigenvalue that satisfies the condition

$$m > m_c = \frac{1-n}{n+1} = 0. \tag{31}$$

Thus, system (30) leads to the following general solution for $F(r,\theta)$:

$$F(r,\theta) = \left(C_1 r^m + C_2 r^{-m}\right)[A\cos(m\theta) + B\sin(m\theta)], \qquad m > 0. \tag{32}$$

Following [2,24] and recalling (28), we rewrite the boundary conditions as

- For antisymmetric flows,

$$\Theta'(\alpha) = 0, \quad \text{and} \quad \Theta(0) = 0, \tag{33}$$

- For symmetric flows,

$$\Theta'(\alpha) = 0, \quad \text{and} \quad \Theta'(0) = 0, \tag{34}$$

and we require that for $r = 0$, the solution is bounded, i.e., $R(r) = C_1 r^m$. Therefore, the solution is

- For antisymmetric flows,

$$F(r,\theta) = r^{m_a} \sin(m_a\theta), \quad m_a = \frac{k\pi}{2\alpha}, \tag{35}$$

- For symmetric flows,

$$F(r,\theta) = r^{m_s} \cos(m_s\theta), \quad m_s = \frac{k\pi}{\alpha}, \tag{36}$$

where the smallest eigenvalues m_a and m_s are obtained for $k = 1$, and we set the constants of integration (C_1, A, B) equal to (1, 0, 1) for antisymmetric flows and (C_1, A, B) equal to (1, 1, 0) for symmetric flows. As the expression of the dependence of viscosity on pressure is given, we can obtain the pressure field through (28), i.e., by solving with respect to $p(r,\theta)$, as follows:

$$F(r,\theta) = \int_0^{p(r,\theta)} \frac{ds}{f(s)}. \tag{37}$$

Application to the Case of Viscosity Given by (14)

In this Subsection, we analyze the case of pressure-dependent viscosity given by (14), showing that (37) has an exact solution. If the viscosity is given by (14), one gets

- For antisymmetric flows,

$$p(r,\theta) = -\frac{\ln|1 - r^{m_a}\delta \sin(m_a\theta)|}{\delta}, \quad m_a = \frac{\pi}{2\alpha}, \tag{38}$$

- For symmetric flows,

$$p(r,\theta) = -\frac{\ln|1 - r^{m_s}\delta \cos(m_s\theta)|}{\delta}, \quad m_s = \frac{\pi}{\alpha}, \tag{39}$$

For the classical Newtonian case, i.e., when the viscosity is given by (14) with $\delta \to 0$, we retrieve

- For antisymmetric flows,

$$p(r,\theta) = r^{m_a} \sin(m_a\theta) \quad m_a = \frac{\pi}{2\alpha}, \tag{40}$$

- For symmetric flows,

$$p(r,\theta) = r^{m_s} \cos(m_s\theta), \quad m_s = \frac{\pi}{\alpha}, \tag{41}$$

as in [24].

The solution of the pressure field and the corresponding evolution of pressure-dependent viscosity for both antisymmetric and symmetric flows when $\alpha = \pi/3, 3\pi/4$ and for different values of δ are depicted in Figures 4–7. In particular, we see that the pressure field p and the viscosity $f(p)$ increase as δ increases in both geometries (non re-entrant and re-entrant angles) and for both type of flows (antisymmetric and symmetric).

The components of the fluxes q_u and q_v for antisymmetric and symmetric flows decrease as δ increases when $\alpha = \pi/3$ and $\alpha = 3\pi/4$, as shown in Figures 8 and 9, respectively. The classical Newtonian case corresponds to $\delta \to 0$. The flow towards the non re-entrant angle $\alpha = \pi/3$ is depicted in Figure 8. In particular, the results highlight

that (q_u, q_v) is decreasing near the corner in the case of antisymmetric and symmetric flows. On the other hand, Figure 9 shows the increase in (q_u, q_v) near the corner in the case of antisymmetric and symmetric flows when $\alpha = 3\pi/4$. Moreover, the flow is distributed unevenly near the bend when the flow is antisymmetric in both geometries, i.e., for both $\alpha = \pi/3$ and $\alpha = 3\pi/4$. The behavior of both flows is different when non re-entrant or re-entrant angles are considered for a given δ. However, in both geometries (non re-entrant and re-entrant angles), the components of the fluxes q_u and q_v in both cases of antisymmetric and symmetric flows decrease as δ increases.

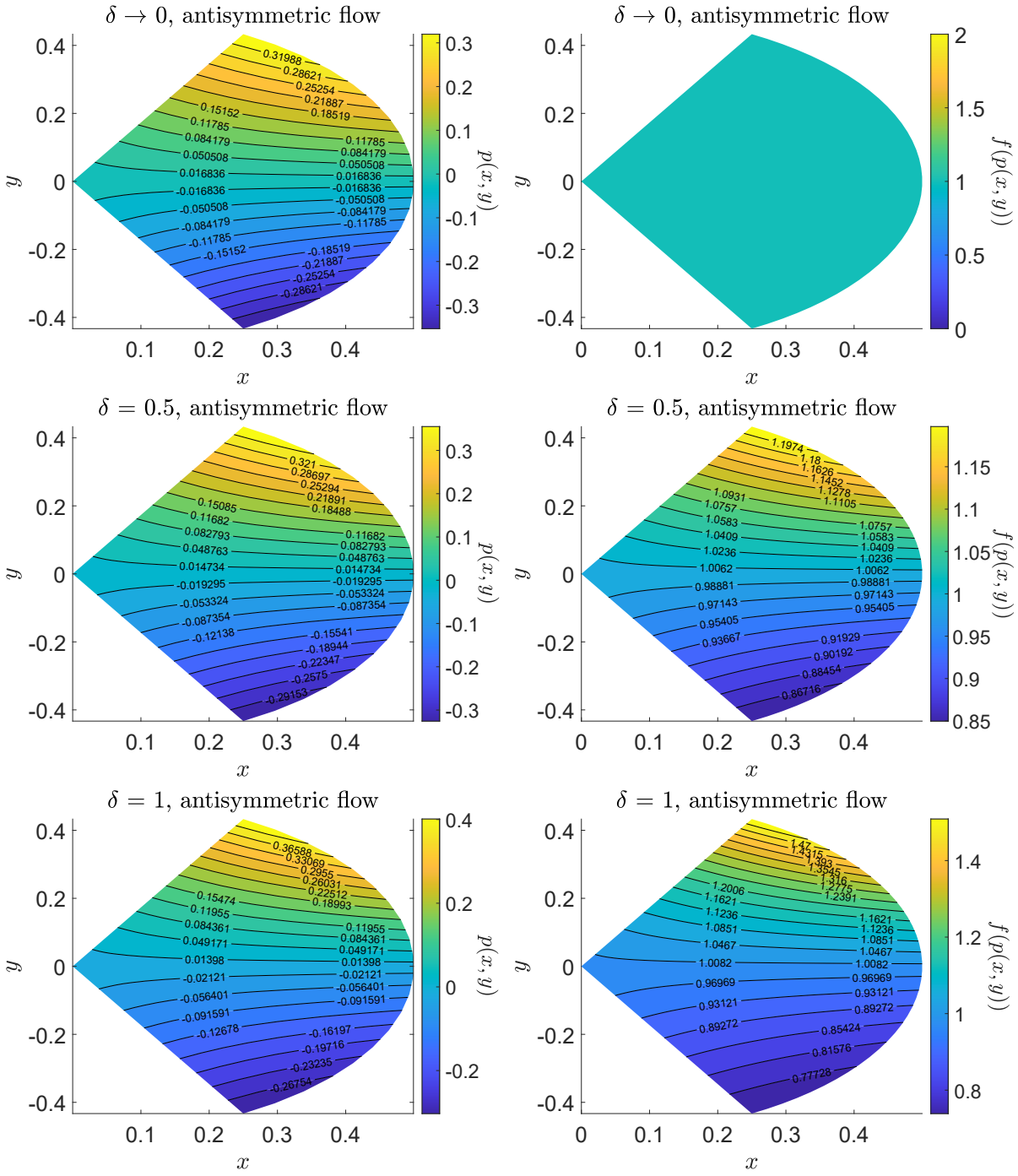

Figure 4. Plots of the pressure field (**left**) and of the viscosity given by (14) (**right**) in Cartesian coordinates for $\delta \to 0$ (i.e. classical Newtonian fluid) and for $\delta = 0.5, 1$ (i.e. piezo−viscous fluid) in the case of antisymmetric flows when $\alpha = \pi/3$.

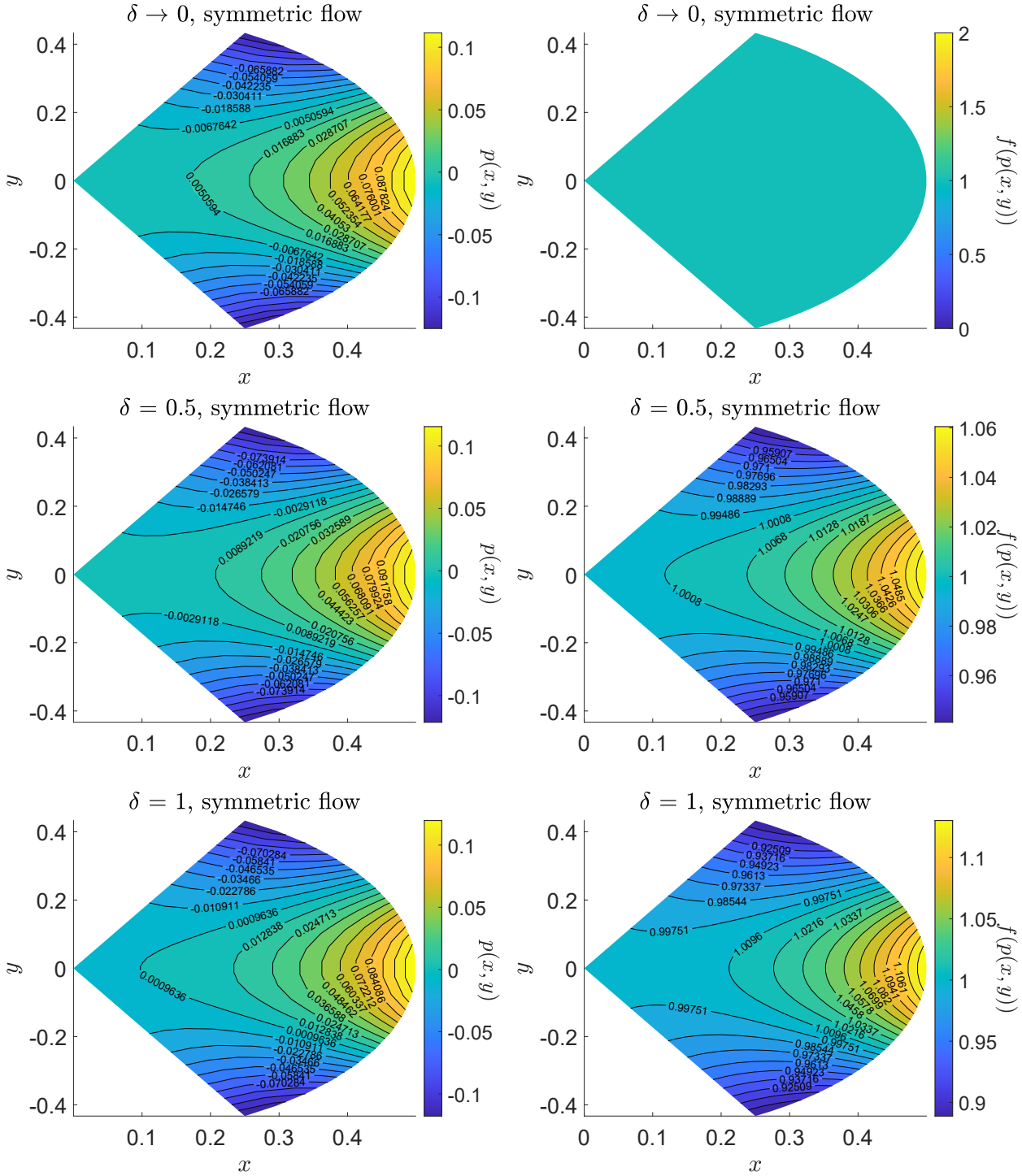

Figure 5. Plots of the pressure field (**left**) and of the viscosity given by (14) (**right**) in Cartesian coordinates for $\delta \to 0$ (i.e. classical Newtonian fluid) and for $\delta = 0.5, 1$ (i.e. piezo−viscous fluid) in the case of symmetric flows when $\alpha = \pi/3$.

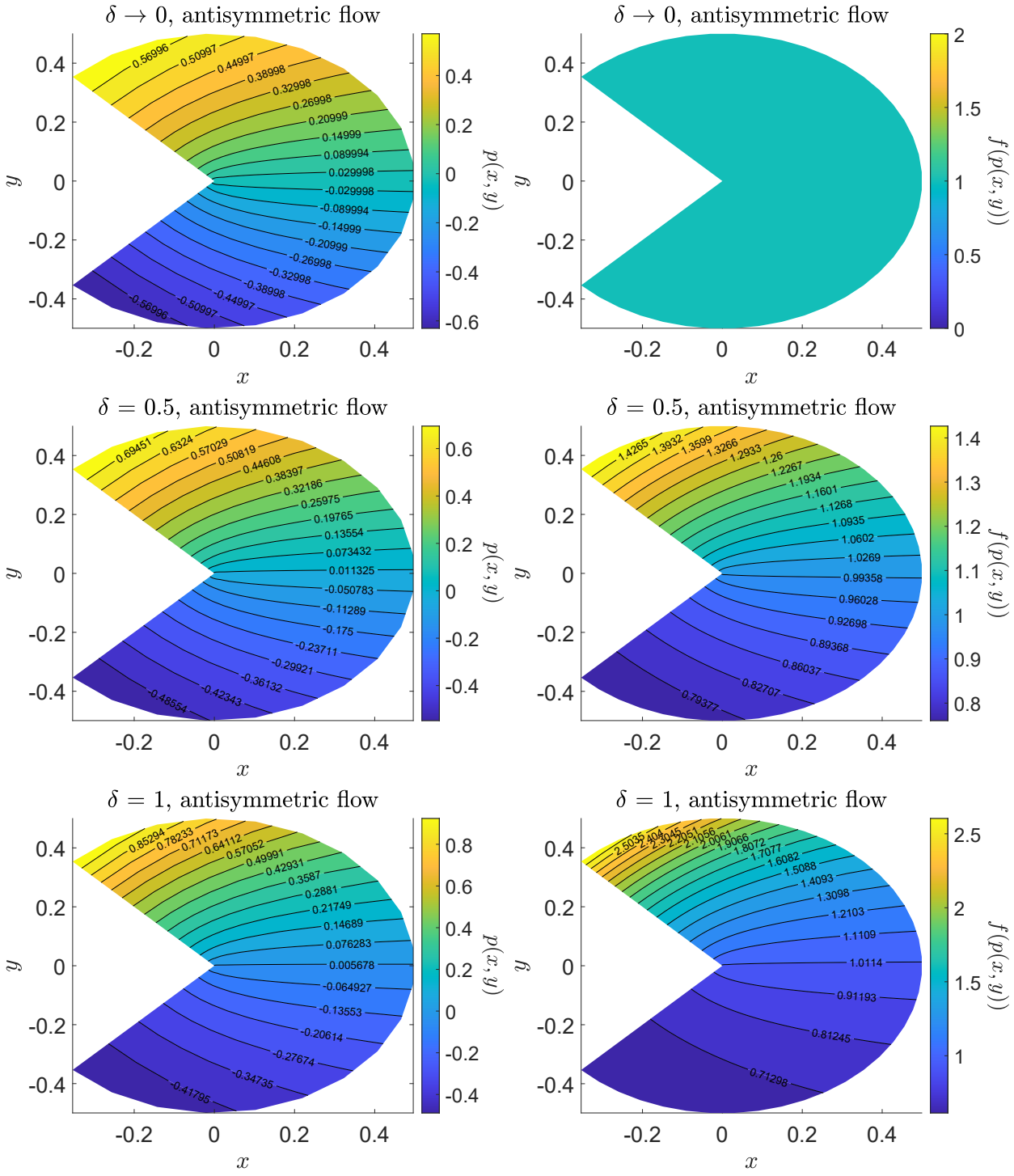

Figure 6. Plots of the pressure field (**left**) and of the viscosity given by (14) (**right**) in Cartesian coordinates for $\delta \to 0$ (i.e. classical Newtonian fluid) and for $\delta = 0.5, 1$ (i.e. piezo−viscous fluid) in the case of antisymmetric flows when $\alpha = 3\pi/4$.

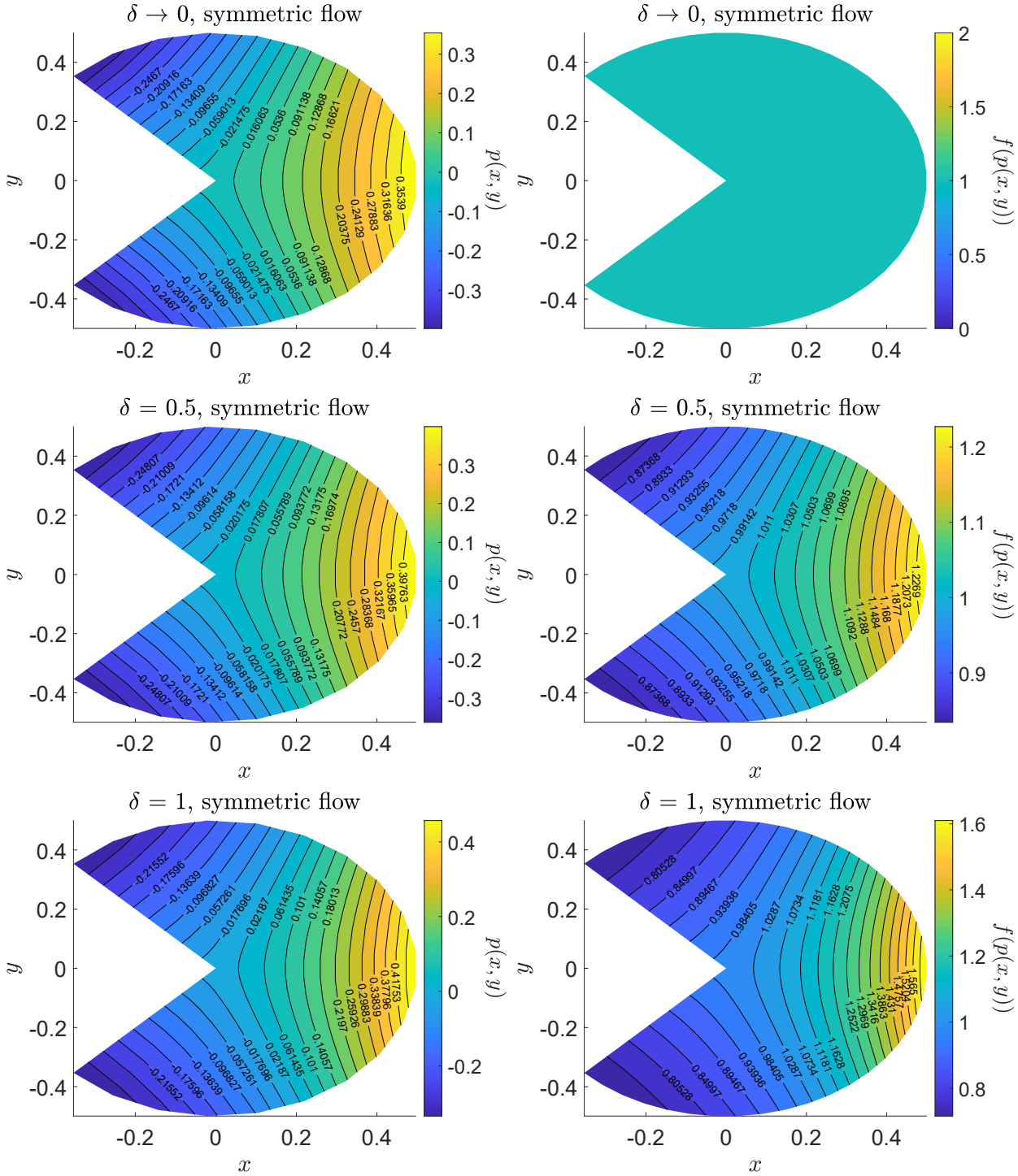

Figure 7. Plots of the pressure field (**left**) and of viscosity given by (14) (**right**) in Cartesian coordinates for $\delta \to 0$ (i.e. classical Newtonian fluid) and for $\delta = 0.5, 1$ (i.e. piezo−viscous fluid) in the case of symmetric flows when $\alpha = 3\pi/4$.

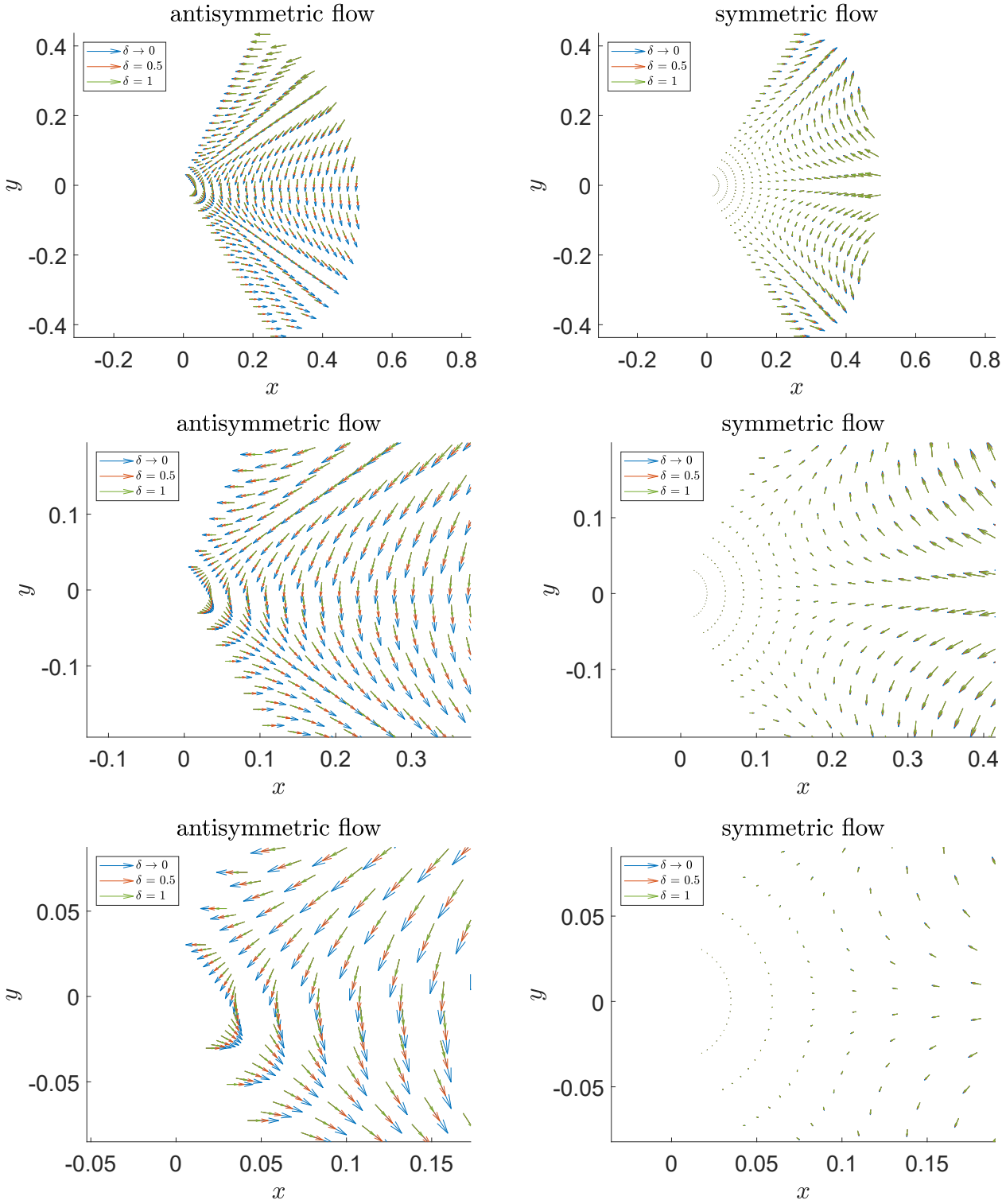

Figure 8. Comparison of fluxes in Cartesian coordinates for classical Newtonian fluid (i.e. $\delta \to 0$) and piezo−viscous fluid with the viscosity given by (14) for $\delta = 0.5, 1$ in the case of antisymmetric (**left**) and symmetric (**right**) flows when $\alpha = \pi/3$. The corresponding magnification is reported from the maximum to the minimum value.

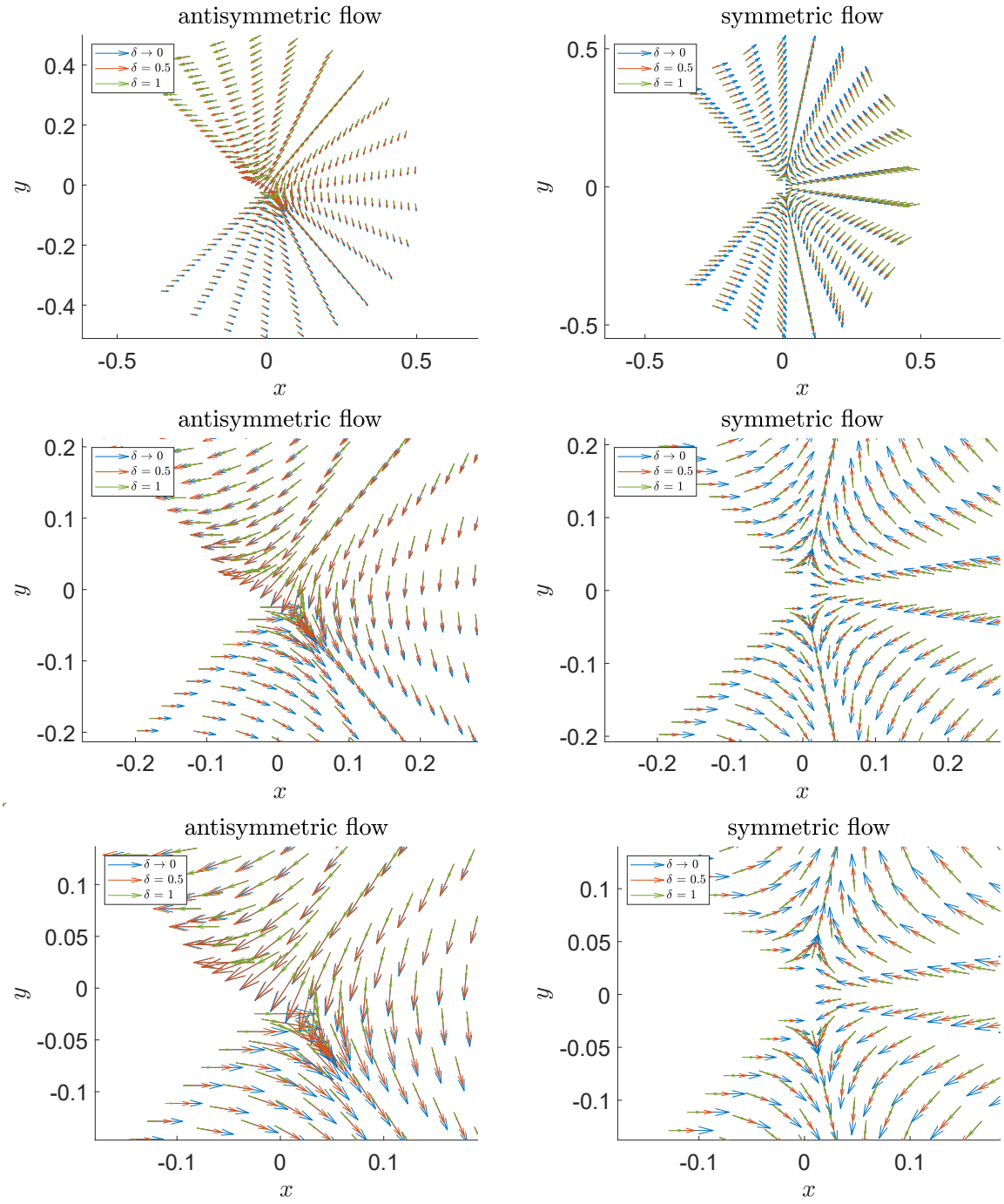

Figure 9. Comparison of fluxes in Cartesian coordinates for classical Newtonian fluid (i.e. $\delta \to 0$) and piezo−viscous fluid with the viscosity given by (14) for $\delta = 0.5, 1$ in the case of antisymmetric (**left**) and symmetric (**right**) flows when $\alpha = 3\pi/4$. The corresponding magnification is reported from the maximum to the minimum value.

4. Conclusions

In this work, we investigated the Hele-Shaw flow of fluids whose viscosity depends on pressure, i.e., piezo-viscous fluids. In particular, we analyzed the case of both antisymmetric (perpendicular to the edge axis of symmetry) and symmetric (directed towards the edge and parallel to its axis of symmetry) flows. We proceeded similarly to [2], and we provided a procedure based on the method of separation of variables to obtain the solution of the pressure field without the dependence on a specific relation between viscosity and pressure.

We report results for the case of an exponential dependence of viscosity on pressure (Barus' law [28]) as an example of exact solutions for the pressure field. In this case, we present the solutions for the pressure field (p), the viscosity ($f(p)$), and fluxes (q_u and q_v) by varying the numerical value of the "material" and geometrical parameter δ, which is related to the pressure coefficient δ^*. Moreover, we analyze such solutions in the area of both non re-entrant ($\alpha = \pi/3$) and re-entrant angles ($\alpha = 3\pi/4$). The solution of the classical Newtonian fluid was recovered when $\delta \to 0$, as in [24]. In particular, our work provides a method to model the behavior of a fluid with pressure-dependent viscosity in Hele-Shaw flows.

Important future extensions of the present work encompass the active control of Hele-Shaw cells by considering the moving fluid interface and the influence of adjustments in gap thickness and inlet pressure. A strategy for controlling the fingering pattern is the use of non–Newtonian fluids as the displaced and/or displacing fluids [14]. The interest in viscous fingering in Hele-Shaw cells is increasing, and the viscous fingering control method is quite attractive for applications regarding interfacial instabilities. In fact, recently, new theoretical, numerical, and experimental studies have been performed regarding the problem of optimally filling a Hele-Shaw cell (e.g., see [14–16,18]).

Therefore, knowledge about fluid characteristics such as the dependence of viscosity upon temperature and/or on the shear rate $\dot{\gamma}$ will be beneficial to better understand geophysical phenomena or to optimize industrial manufacturing.

Author Contributions: Conceptualization, B.C. and L.I.P.; methodology, B.C. and L.I.P.; software, B.C.; formal analysis, B.C. and L.I.P.; investigation, B.C. and L.I.P.; writing—original draft preparation, B.C.; writing—review and editing, B.C. and L.I.P. All authors have read and agreed to the published version of the manuscript.

Funding: Partial funding was provided by the Institut Camille Jordan CNRS UMR 5208 through a grant awarded to Liviu Iulian Palade. Also, this research was equally performed under the auspices of the Italian National Group for Mathematical Physics (GNFM-Indam) and was carried out under the framework of PRIN 2022 project "Mathematical modelling of heterogeneous systems" and the National Recovery and Resilience Plan, Mission 4 Component 2—Investment 1.4—NATIONAL CENTER FOR HPC, BIG DATA AND QUANTUM COMPUTING—funded by the European Union—NextGenerationEU—CUP B83C22002830001).

Data Availability Statement: Data are contained within this article.

Conflicts of Interest: The authors declare no conflicts of interest.

References

1. Aronsson, G.; Janfalk, U. On Hele–Shaw flow of power-law fluids. *Eur. J. Appl. Math.* **1992**, *3*, 343–366. [CrossRef]
2. Chupin, L.; Palade, L.I. Generalized Newtonian and Herschel–Bulkley yield stress fluids pressure behavior near the tip of a sharp edge in thin film flows. *Phys. Lett. A* **2008**, *372*, 6404–6411. [CrossRef]
3. Allouche, M.H.; Millet, S.; Botton, V.; Henry, D.; Hadid, H.B.; Rousset, F. Stability of a flow down an incline with respect to two-dimensional and three-dimensional disturbances for Newtonian and non-Newtonian fluids. *Phys. Rev. E* **2015**, *92*, 063010. [CrossRef] [PubMed]
4. Allouche, M.H.; Botton, V.; Millet, S.; Henry, D.; Dagois-Bohy, S.; Güzel, B.; Hadid, H.B. Primary instability of a shear-thinning film flow down an incline: Experimental study. *J. Fluid Mech.* **2017**, *821*, R1. [CrossRef]
5. Balmforth, N.J.; Liu, J.J. Roll waves in mud. *J. Fluid Mech.* **2004**, *519*, 33–54. [CrossRef]
6. Benjamin, T.B. Wave formation in laminar flow down an inclined plane. *J. Fluid Mech.* **1957**, *2*, 554. [CrossRef]
7. Borsi, I.; Farina, A.; Fasano, A.; Rajagopal, K.R. Modelling the combined chemical and mechanical action for blood clotting. *Nonlinear Phenom. Energy Dissipation Gakuto Int. Ser. Math. Sci. Appl. Gakkotosho Tokyo* **2008**, *29*, 53–72.
8. Calusi, B.; Fusi, L.; Farina, A. On a free boundary problem arising in snow avalanche dynamics. *ZAMM J. Appl. Math. Mech. Z. Angew. Math. Mech.* **2015**, *96*, 453–465. [CrossRef]
9. Calusi, B.; Farina, A.; Fusi, L.; Palade, L.I. Stability of a Regularized Casson Flow down an Incline: Comparison with the Bingham Case. *Fluids* **2022**, *7*, 380. [CrossRef]
10. Calusi, B.; Fusi, L.; Farina, A. Linear stability of a Couette flow for non-monotone stress-power law models. *Eur. Phys. J. Plus* **2023**, *138*, 933. [CrossRef]

11. Calusi, B.; Farina, A.; Fusi, L.; Rosso, F. Thermo-mechanical modeling of pancakelike domes on Venus. *Phys. Fluids* **2024**, *36*, 056607. [CrossRef]
12. Chakraborty, S.; Sheu, T.W.H.; Ghosh, S. Dynamics and stability of a power-law film flowing down a slippery slope. *Phys. Fluids* **2019**, *31*, 013102. [CrossRef]
13. Farina, A.; Fusi, L. Viscoplastic Fluids: Mathematical Modeling and Applications. In *Non-Newtonian Fluid Mechanics and Complex Flows: Levico Terme, Italy 2016*; Farina, A., Mikelić, A., Rosso, F., Eds.; Springer International Publishing: Cham, Switzerland, 2018; pp. 229–298. [CrossRef]
14. Gholinezhad, S.; Kantzas, A.; Bryant, S.L. Control of interfacial instabilities through variable injection rate in a radial Hele-Shaw cell: A nonlinear approach for late-time analysis. *Phys. Rev. E* **2023**, *107*, 065108. [CrossRef] [PubMed]
15. Hintermüller, M.; Keil, T. Optimal control of geometric partial differential equations. In *Geometric Partial Differential Equations—Part II*; Elsevier: Amsterdam, The Netherlands, 2021; pp. 213–270. [CrossRef]
16. Li, P.; Huang, X.; Zhao, Y.P. Active control of electro-visco-fingering in Hele-Shaw cells using Maxwell stress. *iScience* **2022**, *25*, 105204. [CrossRef] [PubMed]
17. Pascal, J.P. Linear stability of fluid flow down a porous inclined plane. *J. Phys. D Appl. Phys.* **1999**, *32*, 417–422. [CrossRef]
18. Petit, N. Optimal control of viscous fingering. *J. Process Control* **2024**, *135*, 103150. [CrossRef]
19. Rajagopal, K.R.; Saccomandi, G.; Vergori, L. Flow of fluids with pressure- and shear-dependent viscosity down an inclined plane. *J. Fluid Mech.* **2012**, *706*, 173–189. [CrossRef]
20. Falsaperla, P.; Giacobbe, A.; Mulone, G. Stability of the Plane Bingham–Poiseuille Flow in an Inclined Channel. *Fluids* **2020**, *5*, 141. [CrossRef]
21. Fernández-Nieto, E.D.; Noble, P.; Vila, J.P. Shallow Water equations for Non-Newtonian fluids. *J. Non-Newton. Fluid Mech.* **2010**, *165*, 712–732. [CrossRef]
22. Fusi, L. Channel flow of viscoplastic fluids with pressure-dependent rheological parameters. *Phys. Fluids* **2018**, *30*, 073102. [CrossRef]
23. Hele-Shaw, H.S. The Flow of Water. *Nature* **1898**, *58*, 34–36. [CrossRef]
24. Hassager, O.; Lauridsen, T.L. Singular behavior of power–law fluids in Hele–Shaw flow. *J. Non-Newton. Fluid Mech.* **1988**, *29*, 337–346. [CrossRef]
25. Hieber, C.; Shen, S. A finite-element/finite-difference simulation of the injection-molding filling process. *J.-Non-Newton. Fluid Mech.* **1980**, *7*, 1–32. [CrossRef]
26. Huilgol, R. On the derivation of the symmetric and asymmetric Hele–Shaw flow equations for viscous and viscoplastic fluids using the viscometric fluidity function. *J. Non-Newton. Fluid Mech.* **2006**, *138*, 209–213. [CrossRef]
27. Ouyang, Y.; Md Basir, M.F.; Naganthran, K.; Pop, I. Unsteady magnetohydrodynamic tri-hybrid nanofluid flow past a moving wedge with viscous dissipation and Joule heating. *Phys. Fluids* **2024**, *36 062009*. [CrossRef]
28. Barus, C. Isothermals, isopiestics and isometrics relative to viscosity. *Am. J. Sci.* **1893**, *s3–45* , 87–96. [CrossRef]
29. Bridgman, P. *The Physics of High Pressure*; The Macmillan Compan: New York, NY, USA, 1931.
30. Fusi, L.; Tozzi, R. Falkner–Skan boundary layer flow of a fluid with pressure-dependent viscosity past a stretching wedge with suction or injection. *Int. J. Non-Linear Mech.* **2024**, *163*, 104746. [CrossRef]
31. Klettner, C.; Dang, T.; Smith, F. On the flow past ellipses in a Hele-Shaw cell. *J. Fluid Mech.* **2023**, *971*, A12. [CrossRef]
32. Kondic, L.; Palffy-Muhoray, P.; Shelley, M.J. Models of non-Newtonian Hele-Shaw flow. *Phys. Rev. E* **1996**, *54*, R4536–R4539. [CrossRef]
33. Nassehi, V. Generalized Hele-Shaw models for non-Newtonian, nonisothermal flow in thin curved layers. *IMA J. Manag. Math.* **1996**, *7*, 71–88. [CrossRef]
34. Rajagopal, K.R. On Implicit Constitutive Theories. *Appl. Math.* **2003**, *48*, 279–319. [CrossRef]
35. Rajagopal, K.R.; Saccomandi, G.; Vergori, L. Stability analysis of the Rayleigh–Bénard convection for a fluid with temperature and pressure dependent viscosity. *Z. Angew. Math. Phys.* **2009**, *60*, 739–755. [CrossRef]
36. Rajagopal, K.; Saccomandi, G.; Vergori, L. On the Oberbeck–Boussinesq approximation for fluids with pressure dependent viscosities. *Nonlinear Anal. Real World Appl.* **2009**, *10*, 1139–1150. [CrossRef]
37. Saccomandi, G.; Vergori, L. Piezo-viscous flows over an inclined surface. *Q. Appl. Math.* **2010**, *68*, 747–763. [CrossRef]
38. Hron, J.; Málek, J.; Rajagopal, K.R. Simple flows of fluids with pressure–dependent viscosities. *Proc. R. Soc. Lond. Ser. A. Math. Phys. Eng. Sci.* **2001**, *457*, 1603–1622. [CrossRef]
39. Rajagopal, K.; Saccomandi, G.; Vergori, L. Unsteady flows of fluids with pressure dependent viscosity. *J. Math. Anal. Appl.* **2013**, *404*, 362–372. [CrossRef]